RAPID PUBLICATION

Long-term Intermittent Hypoxia in Mice: Protracted Hypersomnolence with Oxidative Injury to Sleep-Wake Brain Regions

Sigrid C. Veasey, MD[1,2]; Christine W Davis, MD[3]; Polina Fenik, MS[1,2]; Guanxia Zhan, MD[1,2]; Yeou-Jey Hsu, BS[1]; Domenico Pratico, PhD[4]; Andrew Gow, PhD[3]

[1]Center for Sleep & Respiratory Neurobiology, [2]Department of Medicine, [3]Stokes Research Institute, Department of Pediatrics, [4]Center for Experimental Therapeutics, University of Pennsylvania School of Medicine, Philadelphia, PA

Study Objectives: This study was designed to test the hypothesis that long-term intermittent hypoxia (LTIH), modeling the hypoxia-reoxygenation events of sleep apnea, results in oxidative neural injury, including wake-promoting neural groups, and that this injury contributes to residual impaired maintenance of wakefulness.

Design: Sleep times and oxidative-injury parameters were compared for mice exposed to LTIH and mice exposed to sham LTIH.

Subjects: Adult male C57BL/6J mice were studied.

Interventions: Mice were exposed to LTIH or sham LTIH in the lights-on period daily for 8 weeks. Electrophysiologic sleep-wake recordings and oxidative-injury measures were performed either immediately or 2 weeks following LTIH exposures.

Measurements and Results: At both intervals, total sleep time per 24 hours in LTIH-exposed mice was increased by more than 2 hours, ($P<.01$). Mean sleep latency was reduced in LTIH-exposed mice relative to sham LTIH mice (8.9 ± 1.0 minutes vs 12.7 ± 0.5 minutes, respectively, $P<.01$). Oxidative injury was present 2 weeks following LTIH in wake-promoting regions of the basal forebrain and brainstem: elevated isoprostane 8,12-iso-IPF$_{2\alpha}$-VI, 22%, $P<.05$; increased protein carbonylation, 50%, $P<.05$, increased nitration, 200%, $P<.05$, and induction of antioxidant enzymes glutathione reductase and methionine sulfoxide reductase A, $P<.01$.

Conclusions: Exposure to LTIH results in an array of significant oxidative injuries in sleep-wake regions of the brain, and these biochemical changes are associated with marked hypersomnolence and increased susceptibility to short-term sleep loss. The residual forebrain redox alterations in wake-promoting brain regions may contribute to persistent sleepiness in a prevalent disorder, obstructive sleep apnea.

Key Words: oxidation, oxidative stress, wakefulness, hypoxia, apnea

Citation: Veasey SC; Davis CW; Fenik P et al. Long-term intermittent hypoxia in mice: protracted hypersomnolence with oxidative injury to sleep-wake brain regions. *SLEEP* 2004;27(2):194-201.

INTRODUCTION

MORE THAN 5 MILLION ADULT AMERICANS HAVE OBSTRUCTIVE SLEEP APNEA (OSA).[1] Two thirds of adults with OSA complain of significant sleepiness, fatigue, or both.[2] One quarter of patients with OSA have uncontrollable sleepiness that regularly interferes with their quality of life.[1] When treated for OSA, patients typically report less somnolence.[3-5] However, clinical trials assessing the effectiveness of therapy for OSA show significant residual somnolence in many adults despite effective therapy.[3,5-11] Thus, an important clinical question remains unanswered: is the sleepiness in OSA a readily reversible process, or are there lasting alterations in sleep-wake control as a result of the disease process?

OSA involves repeated sleep–state-dependent upper-airway occlusions, typically followed by arousal and complex autonomic responses to disrupted ventilation and upper-airway occlusion.[12]

Numerous physiologic disturbances occur with each obstructive sleep-disordered breathing event, including fluctuations in oxygen and carbon-dioxide tensions, acid-base status, autonomic function, and behavioral state. However, the physiologic derangement most closely associated with sleepiness is the oxygen desaturation severity.[6,13-15] Although the sleep-wake effects of chronic fluctuations in oxygen tension have not been explored, several recent reports indicate that long-term intermittent hypoxia (LTIH), as occurring in OSA, causes profound effects in other neuronal systems, including residual cognitive impairments in rats,[16-18] alterations in the hypoxic ventilatory response,[19] and reduced neuronal excitability in hippocampal CA1 neurons in slice preparations of neonatal mice exposed to LTIH.[20] Therefore, LTIH, independent of the other physiologic disturbances occurring in OSA, may result in residual sleepiness and sleep-wake disturbances.

Several recent studies suggest that LTIH may impose redox alterations in neural tissue.[16-19] Elevated cortical isoprostane levels have been documented in rats after 1 week of intermittent hypoxia (IH).[18] Oxidative neural injury may include not only increased isoprostane formation,[21] but also nitration[22] and carbonylation.[23] It is important, then, in an initial exploration, to determine which major redox pathways are activated and where. Wake-promoting regions, present in the basal forebrain and brainstem (for review[24,25]), are susceptible to oxidative injury.[21-23] In this study, we show that LTIH has long-lasting effects on behavioral state control and that the protracted effects on behavioral state are associated with diverse oxidative alterations throughout the brain but including wake-promoting regions in the basal forebrain and brainstem. Some of these changes, the lipid peroxidation and carbonylation, are considered irreversible biochemical changes.[21,22]

MATERIALS AND METHODS

Animals

Adult (24- to 36-week-old) male C57BL/6J mice (Jackson Laboratory, Bar Harbor, ME) were studied. The methods and study protocols were approved in full by the Institutional Animal Care and Use Committee of the University of Pennsylvania and conformed with the revised NIH Office of Laboratory Animal Welfare Policy. Food and water were provided ad libitum.

LTIH Protocol

The LTIH protocol was adapted from recently published protocols,[16,20] with 2 exceptions: a sham IH (sham LTIH) exposure was incorporated into the protocol, and the duration of exposure to LTIH was 8 weeks to allow for possible adaptive changes, as may be present in OSA.

Disclosure Statement
Support provided by NIH grants HL65225, IIRG-02-4010.

Submitted for publication November 2003
Accepted for publication January 2004
Address correspondence to: Sigrid Carlen Veasey, MD, 987 Maloney Bldg, University of Pennsylvania, 3600 Spruce St, Philadelphia, PA 19104; Fax: (215) 662-7749; E-mail: veasey@mail.med.upenn.edu

Throughout both LTIH and sham LTIH, home cages of mice (4 to a cage) were placed within 1 of 4 Plexiglas chambers (25 inches X 20 inches X 20 inches; Biospherix, Redfield, NY). Flow rates of > 99% pure nitrogen gas and > 99% pure oxygen into the chambers were varied with an automated oxygen profile system (Oxycycler model A84XOV; Biospherix, Redfield, NY) to result in episodic (90-second cycle length) reductions from an ambient oxygen level of 21% to 9% for the LTIH-exposed mice (14%-18% oxyhemoglobin desaturations), where the 9% nadir was maintained for 5 seconds. Central arterial blood gases performed on ketamine/xylazine anesthetized mice (n = 2) in the chamber with the FIO_2 held constant (5 minutes) at 21% and 9% revealed oxyhemoglobin saturation percentages at 93% to 94%, and 77% to 79%, respectively. Sham LTIH was produced with changes in ambient FIO_2 from 21% to 19% over the same cycle length as in the LTIH protocol to provide comparable environmental noise and air exchanges. Both conditions were produced for the majority (10 of 12 hours) of the lights-on period of the 24-hour ambient-light cycle each day of the 8-week exposure. Ambient oxygen, nitrogen, carbon dioxide, humidity, and temperature were recorded throughout study.

Electrode Implantation and Recordings

Following LTIH or sham LTIH, mice were removed from the IH conditions and allowed 1 week under normoxic conditions. A second group of mice was removed from LTIH at the beginning of week 7 for electrode implantation and then placed back into LTIH to complete the 8 weeks. Surgical implantation of electrodes and electrophysiologic recordings followed, using previously described electrode implantation methods.[26] Mice were returned immediately postoperatively to their home cages. Two to 3 days later, mice were placed in individual cages; recording cables were connected to the mice, and the mice were then housed inside a sound-attenuated, shielded, and well-ventilated designated sleep-recording room with a 12-hour lights-on (7:00 AM to 7:00 PM) and 12-hour lights-off schedule (ambient temperature: 25°C ± 2°C). Electroencephalogram (EEG) signals were filtered at 0.3 and 35 Hz (1/2 max, 6 dB/octave), and electromyogram signals were filtered at 1 and 100 Hz and then amplified (12A5, AC amps, Grass Telefactor, West Warwick, RI). Optimal combinations of the frontal and occipital EEG electrodes were acquired with an electrode selector board (12 PB_36 Electrode Selector, Grass). Signals were sent to an A/D board (Converter 4801A, ADAC, Woburn, MA) in standard computers. The behavioral-state acquisition and analysis program used for these studies was ACQ 3.4.[27] Fourier analysis was performed on 10-second epochs of EEG signals (100 Hz digitization). Each 10-second epoch was scored as wake, non-rapid eye movement (NREM) sleep, or rapid eye movement (REM) sleep, and no epochs were excluded from analysis. In all mice included in sleep analysis, the accuracy of the program relative to human-scorer interpretation of raw EEG and integrated electromyogram for > 100 epochs per state was > 95% for waking and NREM sleep and > 85% for REM sleep, as used previously.[26]

Sleep and Sleep Latency Protocols

To quantify sleepiness, a murine multiple sleep latency test (MMSLT) was designed[28] to parallel the human Multiple Sleep Latency Test.[29] Within each of 4 consecutive 30-minute periods, mice were allowed one 20-minute nap opportunity, followed by enforced wakefulness with gentle handling for any behavioral inactivity in the last 10 minutes prior to next nap opportunity. Electrographic recordings were observed for sleep onsets lasting ≥ 30 seconds. Sleep latency for each nap was defined as the latency from the beginning of nap opportunity to sleep onset. MMSLTs were performed from 2:00 PM to 4:00 PM under baseline and 6-hour sleep-loss conditions. The sleep recording and MMSLT protocol were as follows: baseline sleep-wake recordings were initiated 1 week after electrode implantation. Following a 24-hour sleep-wake recording (day 1) and an MMSLT the following day (day 2), mice were deprived of all sleep for the first 6 hours of the lights-on period (day 3) using gentle handling with wakefulness confirmed electrographically. Immediately following the forced wakefulness protocol, a second MMSLT was performed from 2:00 PM to 4:00 PM (day 3). Upon completion of the MMSLT, recovery sleep was recorded for 8 hours (into day 4). Recovery sleep was analyzed in two 4-hour periods following forced wakefulness and the MMSLT; sleep data were compared to the data from the 4-hour baseline period for the same zeitgeber time points.

Sleep and MSLT Analysis

Behavioral state parameters were analyzed using factorial analysis of variance (ANOVA) with Tukey-Kramer *q* corrections for all comparisons or Bonferroni *t* for selected comparisons.[26] The primary variables were total sleep time per 24 hours, NREM sleep time per 24 hours, REM sleep time per 24 hours, and MMSLT values. Two-way ANOVA was used to compare recovery sleep responses in sham LTIH and LTIH mice. Secondary analyses included wake bout length (time spent with consecutive wake epochs following > 30 seconds of sleep), sleep bout length (time spent with consecutive NREM or REM epochs lasting > 30 seconds), diurnal wake ratio (wake time in light relative to dark period), REM sleep latency (onset to REM epoch following at least 3 NREM epochs without intervening wake epochs), arousal index (1 or more wake epochs following at least 3 NREM or REM epochs[26,30]), and delta decline across the rest period (linear slope of relative delta power across hours of the lights on or recovery sleep period[26,31]). Secondary variables were analyzed with 2-way ANOVA, using Tukey-Kramer for multiple pairwise comparisons (*q* values). The Tukey-Kramer *q* value is of similar magnitude to the Bonferroni *t* value and is a conservative statistical tool for multiple comparisons. Values were reported as mean ± SEM. Statistical significance was determined using data analysis software for ANOVA and paired *t* tests (Graph Pad Prism, San Diego, CA) and defined when probabilities of the null hypothesis were < .05.

Measurement of Lipid Peroxidation

Isoprostane (d_4-8,12-*iso*-$iPF_{2\alpha}$-VI) analysis of thalamus and basal forebrain tissue was performed in LTIH (n = 10) and sham LTIH (n = 8) mice following 2-week recovery from IH conditions. Mice were deeply anesthetized with ketamine/xylazine 100/15 mg/kg intraperitoneally and then perfused intracardially with 4°C 0.9% PBS with 2 mmol EDTA and 20mmol BHT, pH 7.4.[32] Brains were immediately removed and placed on a dry-ice dissection block for immediate dissection of the thalamus/basal forebrain. The tissue was weighed and immediately homogenized, and total lipids were extracted using Folch solution (chloroform:methanol 2:1 vol).[33] Base hydrolysis was performed using 15% KOH at 45°C for 1 hour. A fixed amount of internal standard of d_4-8,12-*iso*-$iPF_{2\alpha}$-VI extracted on a C18 cartridge column was added to each sample. Thin-layer chromatography was used for purification of the eluate, and negative-ion chemical ionization gas chromatography-mass spectrometry was used to assay d_4-8,12-*iso*-$iPF_{2\alpha}$-VI. Two-way ANOVA was used to determine group differences.

Immunohistochemistry

Perfusion-fixed brains were flash frozen in liquid nitrogen and then sliced in serial coronal sections (10 μm). For carbonyl immunoreactivity, a modified method of carbonyl derivitization and immunohistochemistry was used.[34,35] In brief, slides blocked of endogenous peroxide (3% H_2O_2 in methanol), progressively hydrated, and exposed to TBS (tris-buffered saline), underwent protein carbonyl derivitization with 2,4-dinitrophenyl hydrazone (DNPH) in HCl for 1 hour at 22°C. Sections were rinsed in TBS, exposed to 10% normal goat serum (NGS) for 30 minutes and rinsed in 1% NGS before incubation with polyclonal rabbit anti-DNPH (Dako, Carpinteria, CA) 1:200 in 1% NGS overnight at 4°C. NGS (1:10) was placed on each slide for 30 minutes at 4°C, rinsed in TBS, and then incubated with peroxidase-labeled goat antirabbit IgG 1:200 with 1% NGS in TBS 1 hour at 22°C. AEC (3-amino-9-ethylcar-

bazole, Sigma) solution was applied for 10 minutes, followed by Hematoxylum. Immunostaining for 3-nitrotyrosine was performed with affinity-purified polyclonal 3-nitrotyrosine (gift of Dr. H. Ischiropolous, University of Pennsylvania, Philadelphia PA), using methods previously described in detail and a dilution of 1:200 and dithionite as a second control with the primary antibody.[36] The magnocellular preoptic region in each mouse was scored for fluorescence intensity relative to background autofluorescence using a scale from 0 to 3, as previously described,[37] with scorers blinded to the condition. Qualitative scores were compared as primary variables for sham LTIH and LTIH, using unpaired 2-tailed *t* testing with Mann-Whitney U-testing for nonparametric data.

Measurement of Oxidized Proteins in the Basal Forebrain

Amounts of oxidized proteins were measured in block dissections of the basal forebrains of mice exposed to either sham LTIH or LTIH using an Oxyblot kit (Intergen, purchase, NY). In brief, 10 μg of protein from SDS extract and 1 × DNPH (20 mmol DNPH in 10% trifluoroacetic acid) were combined for 25 minutes and then neutralized with a 2-M Tris/30% glycerol and 19% 2-mercaptoethanol solution. Samples were electrophoresed on a 10% tris-glycine gel, transferred, and blocked. The blots were incubated overnight with rabbit anti-DNPH antibody (1:150) at 4°C, followed by 1 hour of incubation in goat antirabbit (1:300). Enhanced chemiluminescence (Supersignal; Pierce Biochem; Rockford IL) was used (5 minutes) to detect DNP-conjugated protein with an imaging system (Fluorchem 8900 ImGen Tech New City, NY) and then analyzed with Alphaease® FC Software (Alpha Innotech, San Leandro, CA).

Table 1—Primer and probe sequence sets for selected genes induced in nitrosative and oxidative stress.

Gene	Genbank#	Sequence	Slope of Standard Curve; Linearity correlation
Neuronal nitric oxide	NM 008712	S-AGCTTCCACCTGCCTCGAA AS=GGGCACGGATTCATTCCTT PR=CAGGCACCGGCATCGCTCC	-3.3; 0.99
Hemoxygenase-1	NM 010442	S=GAGGTCAAGCACAGGGTGACA AS=ACGCCATCTGTGAGGGACTCT PR=CCGCCTTCCTGCTCAACATTGA	-3.0; 0.98
Glutathione Reductase 1	NM 010344	S=AAGCGCTTCTCACCCCAGTT AS=GGGTGGCTGAAGACCACAGTA PR=CTGCTGGCCGGAAACTTGCCC	-3.1; 1.00
Methionine Sulfoxide Reductase A	NM 026322	S=GCCAGGAGAGCACAGGGTACT AS=ACATCTAGAGCCAGCAGAGCAAA PR=CCTGCCCTCGGGTGCCCAA	-3.1; 1.00

Note: Shown are sequences for sense (S) and antisense (AS) primers and the Taqman probe (PR) for real-time semiquantification of mRNA copy numbers in micropunches of wake-promoting regions of the basal forebrain, including magnocellular preoptic, substantia inominata, nucleus basalis of Meynert, and horizontal band nuclei. The right column shows slopes and linearity of standard curves, showing excellent sensitivity of primer/probe sets, and suitability for quantification. Minimal copy number detectable for all sets was 100 copies of mRNA.

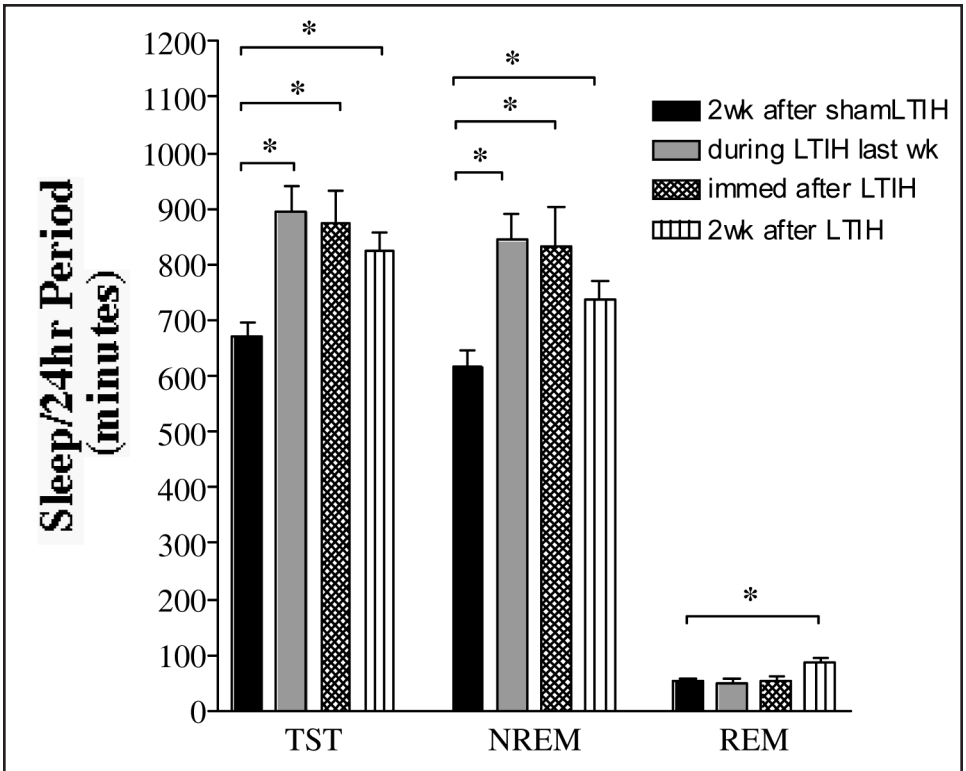

Figure 1—Long-term intermittent hypoxia (LTIH) exposure in mice results in persistent large increases in 24-hour sleep times. Data are shown as average 24-hour sleep times in minutes ± SEM for 4 conditions of long-term intermittent hypoxia: sham LTIH 8 weeks followed by 2-week recovery in normoxia (black bars, n = 9), LTIH 8 weeks, day 56 of exposure, (gray bars, n = 8); LTIH 8 weeks, day 1 recovery, (hatched bars, n = 8); and LTIH 8 weeks, followed by 2 week recovery (striped bars, n = 9). * denotes Bonferroni-corrected differences, relative to sham LTIH data, $P < .05$. For the 3 groups of mice exposed to 8 weeks of LTIH with varying recovery times prior to sleep recordings, there were no differences in total (TST) or non-rapid eye movement (NREM) sleep time for 24 hours. Rapid eye movement (REM) sleep time increased for the 2-week recovery time group, relative to the other groups, $P < .05$.

Antioxidant Transcriptional Response to LTIH

LTIH and sham LTIH mice (n = 5/group) were deeply anesthetized with 80 mg per kg of pentobarbital intraperitoneally and perfused with sterile 4°C PBS. From 500 μm sections of the forebrain macrodissections of the horizontal diagonal band, substantia inominata, nucleus basalis of Meynert and magnocellular preoptic area were collected from each mouse. Methods for mRNA semiquantification have been previously described.[38] Total RNA was extracted by a single step using Tri-zol and chloroform, and PCR amplification was performed in a GeneAmp PCR System 2400 (Perkin Elmer). Standard curves were generated for each primer/probe set using serial dilutions of known quantities of DNA: 100,000, 10,000, 1,000, 100, and 10 copies per well, using methods of Medhurst.[39] Efficiency for each primer/probe set (see Table 1) was quantified as the slope (*m)* of the standard curve ($C_T = m$ (log Q) + c). Quantity of mRNA copies/20 μg total RNA was used as the primary variable for analysis.

RESULTS

LTIH Induces Increased Sleep During and Immediately Following Exposure

Differences in sleep-wake architecture were observed in LTIH mice (n = 8), relative to sham LTIH (n = 9) mice, immediately following 8 weeks of LTIH conditions (F = 59, $P < .001$). On day 1 of return to normoxia, total sleep time in adult mice was 895 ± 55 minutes for LTIH-exposed mice versus 670 ± 30 minutes for Sham LTIH mice, $q = 6.1$, $P < .001$ (Figure 1). The increase in total sleep time was secondary to an isolated increase in NREM sleep (834 ± 100 minutes compared with sham LTIH: 617±27 minutes, $q = 5.1$, $P < .01$). To determine if this increased sleep time might be a

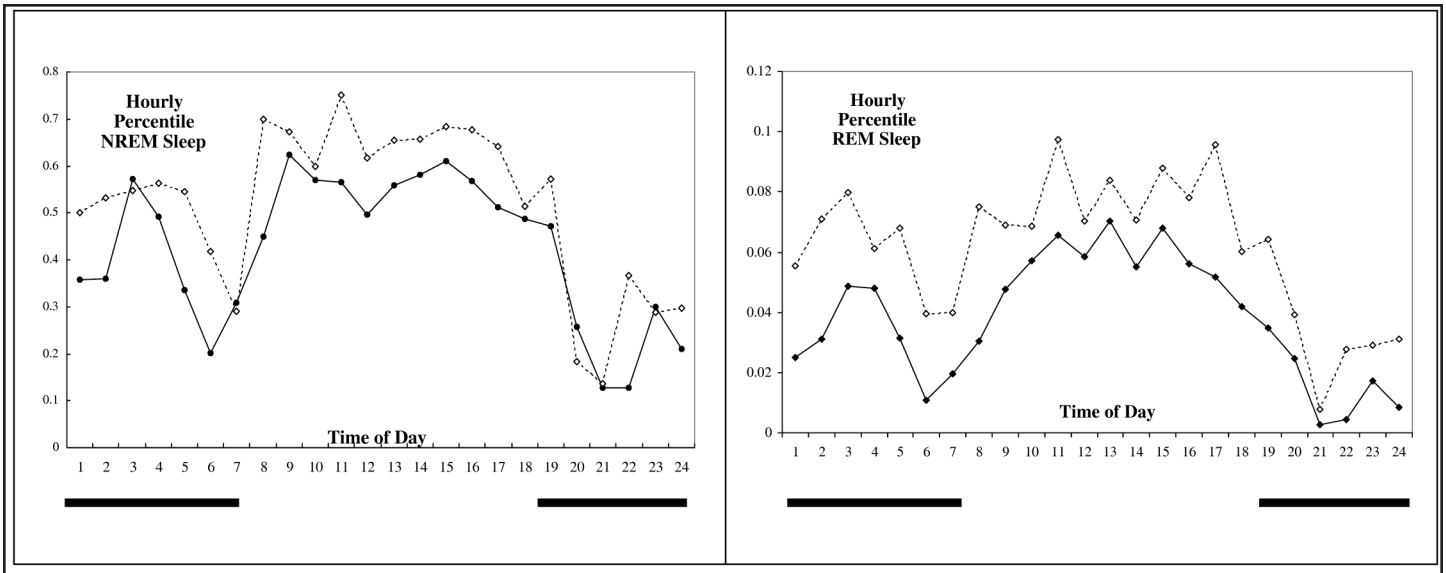

Figure 2—The effects of long-term intermittent hypoxia (LTIH) on hourly sleep-state percentiles across the 24-hour light-dark cycle. Data shown are average hourly sleep-state percentages (percentage of non-rapid eye movement [NREM] sleep/total time, left panel and percentage of rapid eye movement [REM] sleep time/total time, right panel), at 2 weeks normoxia recovery for mice exposed to sham LTIH (closed diamonds) and LTIH (open diamonds). Black bars along the x-axis mark the lights-off period.

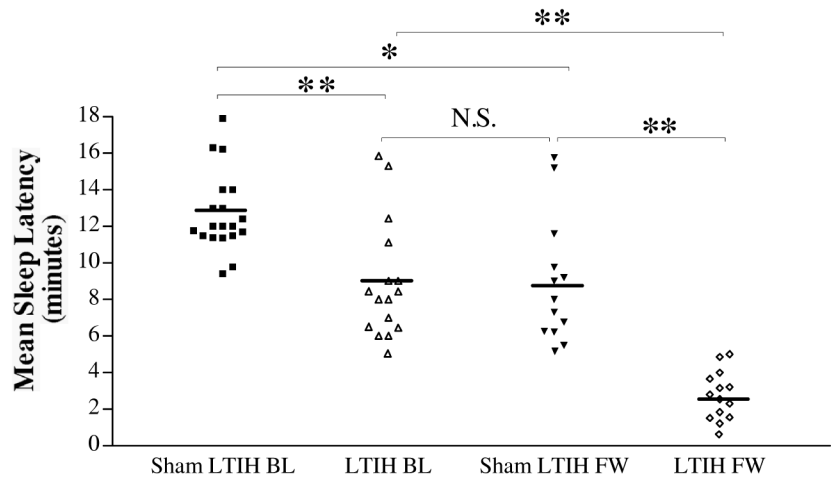

Figure 3—Residual effects of long-term intermittent hypoxia (LTIH) on objective sleepiness. Data shown are individual mean sleep latency values (minutes) obtained using a murine multiple sleep latency test with all data collected from 2:00 PM to 4:00 PM.[28] The black bars on each scattergram denote average sleep latencies for groups of mice exposed to 1 of the 4 LTIH conditions all at the 2-week recovery point: sham LTIH at baseline unperturbed sleep (Sham LTIH BL, closed squares, n = 19); LTIH at baseline unperturbed sleep (LTIH BL, open triangles, n = 16); Sham LTIH after 6 hrs forced wakefulness (Sham LTIH FW, closed triangles, n = 13); and LTIH after 6 hrs forced wakefulness (LTIH FW, open diamonds, n = 14). Although there are overlapping data between groups, there are significant differences between group multiple sleep latency values; * denotes a $P < .01$, and ** denotes a $P < .001$. The sleep latencies for LTIH mice at baseline are similar to the latencies for Sham LTIH mice after 6 hours forced wakefulness in the rest predominant period (lights-on).

rebound phenomenon following poor sleep during LTIH exposure, sleep was measured in this same group of LTIH (n = 9) on the last day of LTIH exposure. Total sleep time per 24 hours was equally elevated in mice during LTIH exposure (NREM sleep and REM sleep were also unchanged, Figure 1). Further, sleep on the last day of LTIH exposure, relative to the first day of normoxia, revealed no differences in arousal index, duration of sleep bouts, or the 24-hour distribution of hourly percentages of NREM and REM sleep.

Effects of LTIH on Sleep Are Protracted

A separate set of mice was examined following a 2-week recovery from either sham LTIH or LTIH. Sleep architecture comparisons between groups, sham LTIH (n = 12) and LTIH (n = 9), revealed significant differences in sleep, F = 59.7, $P < .0001$ (Figure 1). Total sleep time for 24 hours was 156 minutes longer in the LTIH-exposed mice compared to sham LTIH mice, q = 6.8, $P < .001$. NREM sleep was increased by 130 minutes ($q = 5.1$, $P < .001$). REM sleep was higher in all LTIH mice than in sham LTIH mice (27 minutes, Bonferroni $t = 2.7$, $P < .05$). Twenty-four–hour sleep efficiency was increased in the LTIH mice, relative to sham LTIH controls, 71 ± 4% vs 60 ± 1%, Bonferroni $t = 2.9$, $P < .05$. The increase in NREM and REM sleep appeared evenly distributed across the 24-hour cycle (Figure 2). REM-sleep percentage of total sleep per 24 hours was similar for the LTIH and sham LTIH (Bonferroni $t = 0.001$, NS). There were no differences in the relative wakefulness time during dark versus light periods (Bonferroni $t = 0.003$, NS). The arousal index was reduced in the LTIH mice, relative to sham controls (6 ± 2 vs 10 ± 2 arousals per hour, Bonferroni $t = 2.5$, $P < .05$), and a longer average duration for sleep bouts was observed in LTIH mice, 13 ± 1 minutes versus 8 ± 0.5 minutes, Bonferroni $t = 3.3$, $P < .05$. Duration of wakefulness bouts did not differ between LTIH and sham LTIH mice, 8 ± 1 vs. 7 ± 1, respectively, NS

LTIH Results in More Profound Sleepiness Following Short-Term Sleep Loss

Sleep conditions (rested vs after forced wakefulness) and IH conditions (LTIH vs sham LTIH) both affected sleep latencies, F = 38.2, $P < .001$; see Figure 3). Mean sleep latencies differed following undisturbed sleep: 12.7 ± 0.5 minutes, sham LTIH (CI [confidence interval], 9-18 minutes, n = 19) and 8.9 ± 1.0 minutes, LTIH (CI, 4-15 minutes, n = 16), $t = 4.2$, $P < .01$). Following 6 hours of sleep loss, both groups showed reductions in their mean sleep latencies (sham LTIH, 8.9 ± 0.8 minutes, $P < .05$ and LTIH 2.7 ± 0.4 minutes, $P < .01$. However, the mean sleep latencies following sleep loss were significantly lower in LTIH mice compared to sham LTIH mice, $t = 3.5$, $P < .001$.

LTIH Results in Persistent Alterations in Sleep Homeostasis

Short-term sleep loss in sham LTIH mice resulted in increased REM sleep time for both periods in recovery sleep 4:00 PM to 7:00 PM (7 ± 1 minutes baseline and 14 ± 4 minutes recovery, $P < .05$) and 7:00 PM - 10:00 PM (1 ± 0.5 minutes baseline and 5 ± 1 minutes recovery, $P < .05$). In contrast, LTIH mice did not demonstrate an increase in REM sleep following sleep loss for either time period (4:00 PM to 7:00 PM: 11 ± 1 minutes baseline and 12 ± 1 minutes recovery, NS; 7:00 PM - 10:00 PM: 3 ± 0.5 minutes baseline and 6 ±1 minutes recovery, NS. The

delta decline responses are shown in Figure 4. In sham LTIH mice, the slope during recovery sleep was steeper (-5.7) than the slope during unperturbed daytime sleep (-3.2), $t = 3.3$, $P < .01$. In contrast, there was no difference in delta slopes during recovery and baseline sleep (-2.0 during baseline and –2.6 during recovery sleep, $t = 0.8$, NS).

LTIH Results in Redox Alterations

Isoprostane isoform d_4-8,12-*iso*-$iPF_{2\alpha}$-VI (F_2-iP) was increased in homogenates of the thalamus/rostral basal forebrain in mice 14 days after exposure to LTIH: 363 ± 21 pg per mg of protein in LTIH mice (n = 10) and 294 ± 25 pg per mg of protein in sham LTIH mice (n = 7), $P < .03$, as shown in Figure 5. LTIH exposure resulted in an increase in basal forebrain protein carbonylation when measured at the 2-week recovery time point. Total protein carbonylation immunoreactivity (expressed as chemiluminescent density) in homogenates of the rostral basal forebrain in mice exposed to sham LTIH was 34.5% ± 5% compared with 47.7% ± 5% in LTIH, $t = 2.5$, $P < .05$. Examples of enhanced basal forebrain carbonylation following LTIH are presented in Figure 6. Immunohistochemistry of the basal forebrain revealed minimal carbonylation in sham LTIH mice and pronounced carbonylation diffusely in the basal forebrain, including magnocellular, substantia inominata, horizontal diagonal band, median preoptic, and medial septal diagonal band regions of LTIH mice. Many periventricular areas demonstrated increased carbonylation. The median preoptic area showed intense carbonylation in both sham and LTIH mice. The caudate putamen of LTIH mice showed the most intense carbonylation; examples are shown in Figures 7E-H. The hypothalamus revealed weak staining in the lateral hypothalamus, and the hippocampus revealed moderate carbonylation in mice exposed to LTIH. In the brainstem, the periaqueductal gray, red nucleus magnocellular, and dorsal raphe and median raphe showed the most intense carbonylation. In addition, 3-nitrotyrosine immunoreactivity followed the carbonylation patterns overall. Measurement of fluorescence intensity for anti-3-nitrotyrosine relative to background was assessed in the magnocellular preoptic and lateral hypothalamus regions only. Nitration in the magnocellular preoptic region was increased in LTIH mice compared to sham controls, 2.5 ± 0.4 versus 0.7 ± 0.4, U = 32, $P < .05$, as illustrated in Figure 8. There was no increase in nitration in the lateral hypothalamus.

Transcription of antioxidant enzymes increased in the rostral basal forebrain of LTIH mice (n = 6) relative to sham LTIH mice (n = 6), F = 9.3, $P < .01$, as detailed in Figure 9. Although LTIH mice showed higher mean copy numbers, the variance was quite high, and the only statistically significant changes were glutathione reductase (Bonferroni $t = 2.7$, $P < .05$) and methionine sulfoxide reductase A (Bonferroni $t = 4.4$, $P < .001$).

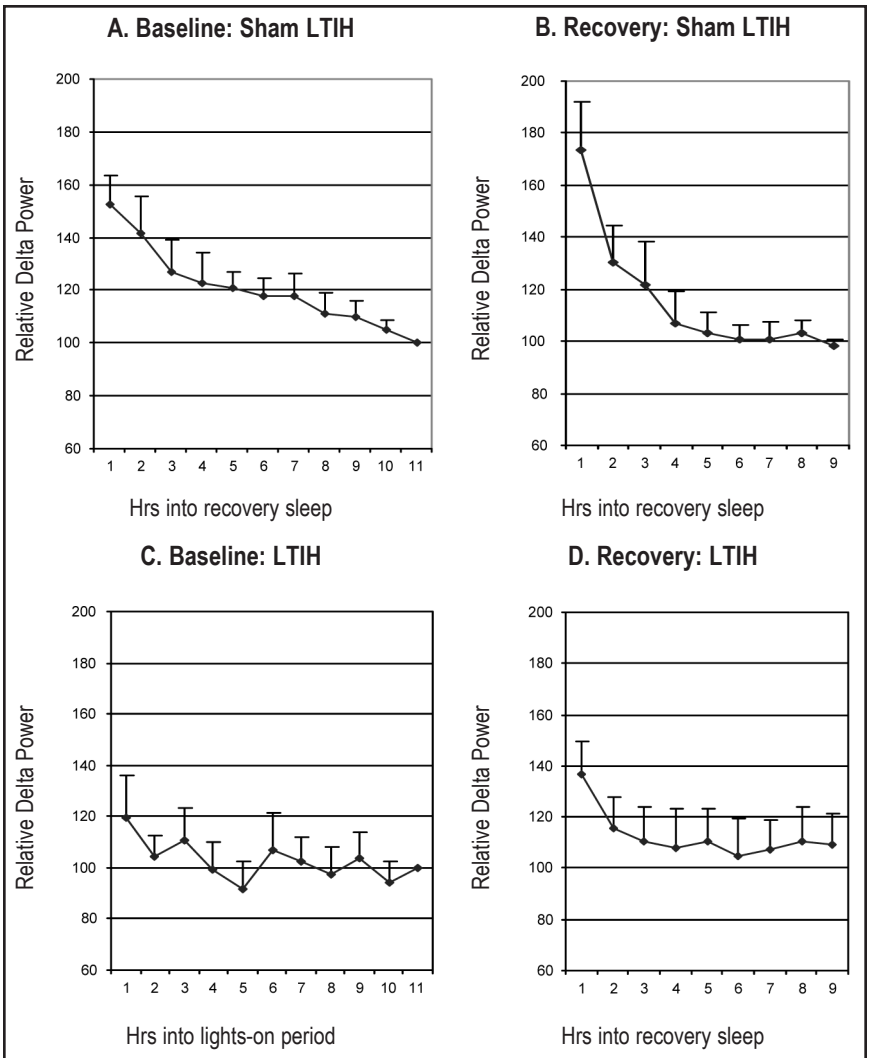

Figure 4—Declines in relative delta power across baseline and recovery sleep in mice exposed to either long-term intermittent hypoxia (LTIH) or sham LTIH. Data are expressed as hourly average delta power values normalized to the last hour of the rest (lights-on) period.[31] Panels A (Sham LTIH) and C (LTIH) show delta decline across the baseline, unperturbed, lights-on period. Panels B (Sham LTIH) and D (LTIH) show the delta decline response after 6 hours of forced wakefulness. Following 6 hours of forced wakefulness, peak relative delta power is increased relative to baseline (Panel A vs B), $P < .05$. In contrast, LTIH mice do not show the expected increase in relative delta power at the beginning of recovery sleep (Panel C vs D).

DISCUSSION

We have identified large and persistent increases in both 24-hour sleep time and objective sleepiness following short-term sleep loss in adult mice under conditions of LTIH. Effects on sleep and sleepiness were present 2 weeks after return to normoxic conditions. In association with the persistent LTIH alterations in behavioral state control, we have observed oxidative changes throughout the brain, including wake-promoting regions of the brainstem and basal forebrain. Specifically, we observed prominent nitration and carbonylation within the magnocellular preoptic, substantia inominata, horizontal diagonal band, the medial septum/vertical diagonal band regions of the basal forebrain, and the lateral hypothalamus, hippocampus, and dorsal raphe nuclei, present 2 weeks after completion of LTIH. Lipid peroxidation and induction of antioxidant enzymes were increased in the basal forebrains of mice exposed to LTIH. Whether these changes occur in other sleep-wake regions will require further study. Together, this work highlights a potential role for intermittent hypoxia in redox injury to the basal forebrain and in the residual sleepiness seen in many patients with OSA. The significant redox alterations induced by LTIH, in the present study, are redox alterations associated with brain injury and many neurodegenerative diseases of the basal forebrain. This work raises the possibility that LTIH, as occurs in OSA, could potentiate oxidative injury in neurodegenerative processes.

Novel Model of OSA Hypersomnolence

By design, the model used for these studies, intermittent hypoxia mimicking severe sleep-disordered breathing, is an incomplete model of OSA. The model includes neither upper-airway obstruction nor hypercapnia, and LTIH does not result in significant sleep fragmentation, as evidenced in this study with sleep recordings during LTIH and immediately following LTIH. Rather, this model with its sham LTIH control, tests the selective contribution of LTIH on neurobehavioral function.[16,20] The hypoxia/reoxygenation condition in the present study models the hypoxia/reoxygenation patterns observed in adults with

severe sleep apnea: oxyhemoglobin desaturations of 14% to 18% occurring 40 times per hour. Thus, this study was designed to explore the importance of severe LTIH/reoxygenation events in the refractory hypersomnolence many persons with OSA experience, despite effective therapy.

A recovery interval of 2 weeks was chosen to look for protracted effects that might explain the significant residual daytime sleepiness in persons treated for OSA.[5] Having shown little recovery at 2 weeks, a longer recovery period will be needed to determine the full extent of reversibility. Consistent with the protracted behavioral-state abnormalities with LTIH, are findings in a recent clinical trial of persons with OSA showing minimal improvement in an abnormal delta decline across sleep within 1 month of therapy, yet significant improvement after many months of therapy.[40] While further studies will be necessary to determine the extent to which alertness is recoverable, the present data suggest that reversal of LTIH-induced sleepiness in persons with severe OSA, if it occurs at all, is unlikely to occur rapidly.

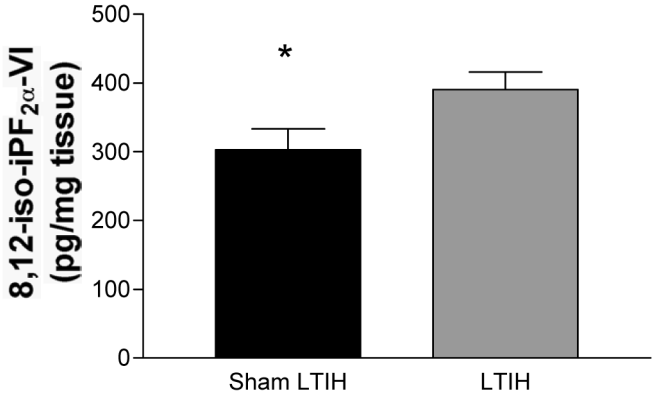

Figure 5—Increased isoprostane (8,12-iso-IPF$_{2\alpha}$-VI) levels in basal forebrain/thalamus homogenates in mice exposed to long-term intermittent hypoxia (LTIH). Shown are mean ± SEM values for sham LTIH (black bar, n = 7) and LTIH (gray bar, n = 10), as measured with gas chromatography – mass spectroscopy revealing increased production of isoprostanes following LTIH exposure. Asterisk * denotes $P < .05$.

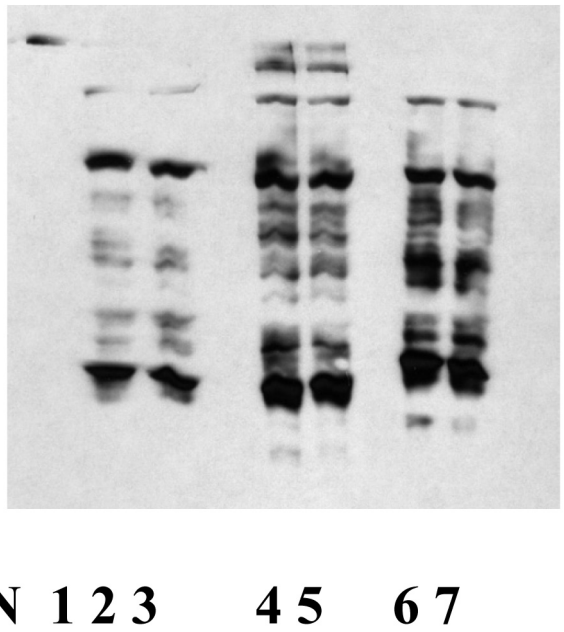

Figure 6—Carbonylation of proteins in the medial and lateral basal forebrain. Representative individual samples of 10 µg of protein isolated from homogenates of the magnocellular preoptic region, vertical and horizontal diagonal bands, and substantia inominata of mice exposed to long-term intermittent hypoxia (LTIH) or sham LTIH. Shown samples were loaded onto a single SDS gel after derivatizing protein with 2,4-dinitrophenyl hydrazone (DNPH) and then exposing samples to polyclonal anti-DNPH for detection of carbonylated proteins.[34,35] Lane 1 is a standard; lanes 2,3 (duplicates) show carbonylation in a sham LTIH mouse. Lanes 4,5 (duplicates form one LTIH mouse and lanes 6,7 (duplicates) for a second LTIH mouse. In all cases a wide range in sizes of proteins show carbonylation. However, bands present in sham LTIH mouse are more dense in LTIH mice and more bands show carbonylation reactivity in LTIH mice.

Mechanisms Underlying LTIH Hypersomnolence

These persistent effects on behavioral-state control following LTIH suggest either neuronal plasticity or injury affecting behavioral-state control mechanisms. Both general processes have been shown to occur

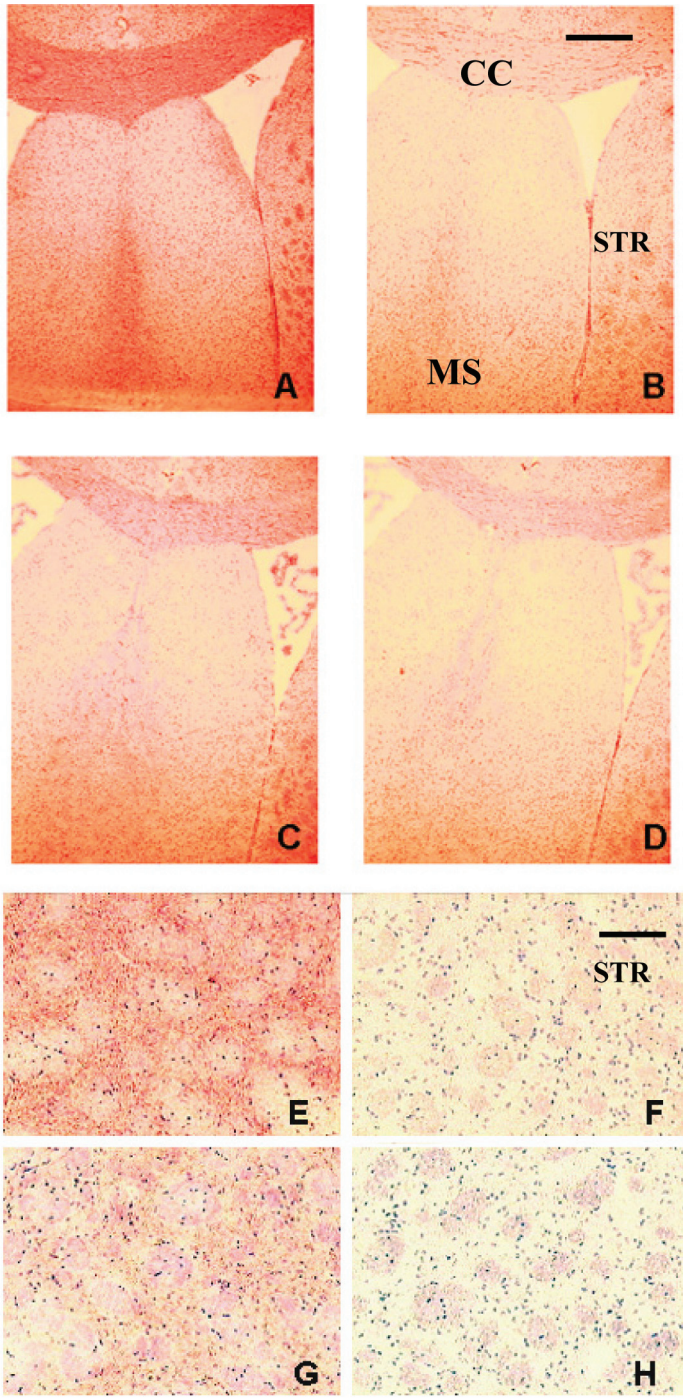

Figure 7—Immunohistochemical detection of protein oxidation throughout the forebrain of mice exposed to long-term intermittent hypoxia (LTIH). Coronal sections (10 µm) exposed immediately to 2,4-dinitrophenyl hydrazone (DNPH) for derivitization of carbonylated proteins were incubated with polyclonal anti-DNPH. Carbonylated proteins are revealed with AEC staining (red). Overall, the most intensely stained regions of the basal forebrain included the medial septum (MS), corpus callosum (CS), and the striatum (STR). Other brain regions with intense staining included the hippocampus and dorsal raphe. Panels A-D, rostral basal forebrain: A = LTIH, anti-DNPH; B = LTIH, no primary; C = sham LTIH, anti-DNPH; D = sham LTIH, no primary; Panels E-H, striatum, high power: E = LTIH, anti-DNPH; F = LTIH, no primary; G = sham LTIH, anti-DNPH; H = sham LTIH, no primary. Bar in A= 1 mm; bar in E = 50 µm.

in non–sleep-wake neuronal populations following IH.[16-20,41,42] Plasticity has been shown following short-term and mild IH.[41,42] Respiratory-drive plasticity has been shown in response to short-term and relatively infrequent IH,[41,42] with phrenic-nerve response to electrical stimulation of the carotid sinus nerve showing long-term facilitation following IH exposures.[42]

Longer-term and more-severe IH has been shown to result in reduced neuronal responsiveness and neural injury.[16-20] LTIH, with IH exposures of similar magnitude to ours, results in increased apoptosis in the hippocampus and cortex and gliosis in the cortex, concordant with impaired spatial learning.[16,18]

Reactive oxygen or nitrogen species, or both, have been implicated in both plasticity and injury responses to IH. Phrenic long-term facilitation may be largely prevented by treatment with a potent superoxide ion scavenger, manganese (III) tetrakis (1-methyl-4-pyridyl) porphyrin pentachloride, throughout exposure to IH.[43] Further, the increased cortical isoprostanes and learning impairments following severe LTIH were largely prevented by treating the rats throughout exposure with a pyrrolopyrimidine antioxidant, PNU-101033E.[18] Together, these data suggest that the production of reactive oxygen species or reactive nitrogen species may contribute to both IH-induced plasticity and neuronal injury.

Following LTIH, immunoreactivity for carbonyl groups and 3-nitrotyrosine was increased throughout the brain and brainstem without a predilection for wake-promoting neuronal groups. The caudate putamen consistently showed the most intense immunoreactivity for carbonylation and nitration. This is consistent with reports of increased vulnerability in the caudate to hypoxia/reoxygenation. Although striatal injury may contribute to sleepiness, a more likely explanation would be the nitration and carbonylation in the magnocellular region and lateral hypothalamus. The increased carbonylation and lipid peroxidation identified in the basal forebrain, hypothalamus, and brainstem following LTIH represent potentially irreversible redox changes,[44-46] and the observed increased 3-nitrotyrosine immunoreactivity and isoprostane levels in this study substantiate peroxynitrite formation.[47,48] Because peroxynitrite has been shown to potentiate vulnerability to oxidative injury,[49,50] we believe that initial injury may increase vulnerability to repeated attacks, as with LTIH. Thus, we hypothesize that the longer the exposure to moderate to severe IH, the more profound the oxidative burden to the brain will be. In contrast, mild IH may offer a preconditioning benefit.[51] The nitrative oxidative burden to the basal forebrain could play an additive role in the development of oxidative neurodegenerative processes.

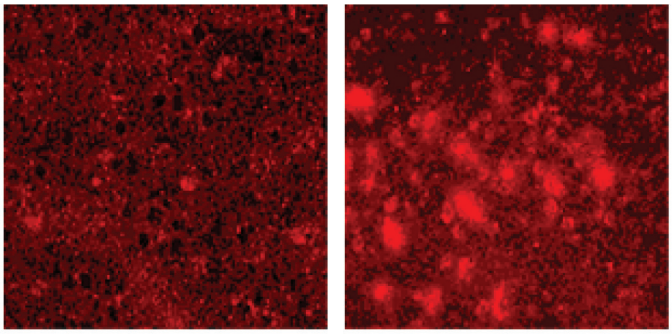

Figure 8—Prominent nitration immunoreactivity in the large cell bodies within the magnocellular preoptic region of a mouse exposed to long-term intermittent hypoxia (LTIH). Immunohistochemical staining performed with a polyclonal antinitrotyrosine antibody and stained with a fluorescent secondary antibody. The left panel reveals baseline fluorescence (no primary control), and the right panel shows the contiguous 10-µm coronal section incubated with the primary anti-3-nitrotyrosine.

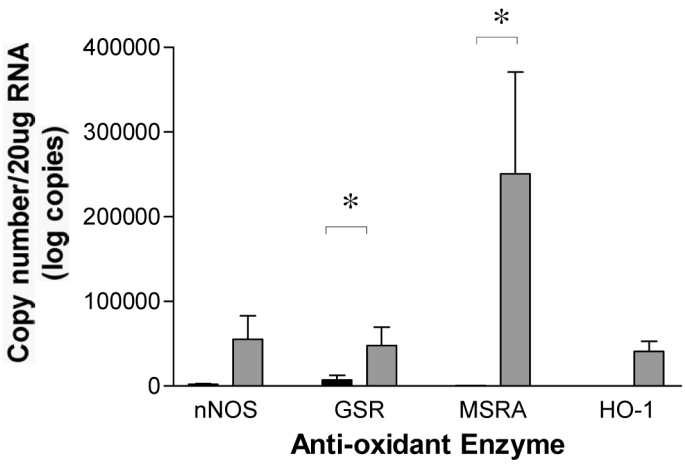

Figure 9— Antioxidant transcriptional response in the basal forebrain to long-term intermittent hypoxia (LTIH). Shown are mean ± SEM mRNA copy numbers from quantitative RT-PCR performed on micropunches (50 laser captures 50-µm diameter) from the magnocellular preoptic region/diagonal band/substantia inominata in mice exposed to sham LTIH (black bars) and LTIH (gray bars). *denotes increases (Bonferroni corrected) in transcription in LTIH samples. NNOS refers to neuronal nitric oxide synthase; GSR, glutathione reductase; MSRA, methionine sulfoxide reductase A; HO-1, hemoxygenase-1.

The pattern of increased total sleep time, evenly distributed across the circadian period, is distinct from the increased sleep patterns recently described in several transgenic murine models of hypersomnolence where increased sleep has been shown only in the initial hours of the dark period.[52-54] Thus, the present findings are not consistent with an isolated alteration in either CREB, or histamine or hypocretin activity. The large increase in NREM sleep and REM sleep, with longer sleep bouts and improved sleep consolidation yet increased sleepiness and impaired delta decline, suggest to us that LTIH affects multiple components of sleep-wake control. The shortened sleep latencies following forced wakefulness suggest that the homeostatic mechanisms are intact. This picture is more consistent with reduced excitability of wake-promoting neurons rather than a loss of cholinergic basal forebrain neurons, where a reduced homeostatic response would be expected. Following short-term enforced wakefulness, mice exposed to IH have an impaired (blunted) delta response in recovery sleep. Abnormalities in delta decline across sleep in persons with OSA have recently been described.[40]

Both reduced activity of wake-promoting neurons or increased activity of sleep-promoting neurons might explain the present findings. Nitration has been shown to activate as well as inactivate important signal transduction enzymes in the basal forebrain,[55-58] including key enzymes for basal forebrain cholinergic neurons.[59] One of the next directions for this work will be to quantify cholinergic and monoaminergic neurons in wake-promoting regions, examine redox injury in these neurons with double-label techniques for cell type and redox injury, and then look at the responsiveness of both wake-promoting and sleep-onset neurons in the basal forebrain to determine the impact of redox alterations on function.

CONCLUDING REMARKS

Together, these findings suggest that the neurobehavioral impairments and the residual sleepiness in persons with OSA may stem from IH-induced high-energy redox alterations in wake-promoting neurons, and that many regions of the brain, including wake-promoting neuronal groups, are susceptible to LTIH oxidative injury. Whether prevention of oxidation or nitration during LTIH or following LTIH can prevent hypersomnolence or facilitate the recovery of alertness will be an important direction for this work to substantiate the relationship between LTIH oxidative injury and residual hypersomnolence. The presented findings may also have implications regarding the hypersomnolence observed in persons with oxidative neurodegenerative disorders, for example, Alzheimer disease,[60] dementia with Lewy bodies,[61] and Parkinson disease[62] and, perhaps, with aging, where oxidative changes have been shown in the cholinergic and monoaminergic collections of wake-promoting neurons.

REFERENCES

1. Young T, Palta M, Dempsey J, Skatrud J, Weber S, Badr S. The occurrence of sleep-disordered breathing among middle-aged adults. N Engl J Med 1993;328:1230-5.
2. Chervin RD. Sleepiness, fatigue, tiredness, and lack of energy in obstructive sleep apnea. Chest 2000;118:372-9.
3. Engleman HM, Martin SE, Kingshott RN, Mackay TW, Deary IJ, Douglas NJ. Randomised placebo controlled trial of daytime function after continuous positive airway pressure (CPAP) therapy for the sleep apnoea/hypopnoea syndrome. Thorax 1998;53:341-5.
4. Morisson F, Decary A, Petit D, Lavigne G, Malo J, Montplaisir J. Daytime sleepiness and EEG spectral analysis in apneic patients before and after treatment with continuous positive airway pressure. Chest 2001;119:45-52.
5. Patel SR, White DP, Malhotra A, Stanchina ML, Ayas NT. Continuous positive airway pressure therapy for treating sleepiness in a diverse population with obstructive sleep apnea:results of a meta-analysis. Arch Int Med 2003;163:565-71.
6. Bedard MA, Montplaisir J, Richer F, Malo J. Nocturnal hypoxemia as a determinant of vigilance impairment in sleep apnea syndrome. Chest 1991;100:367-70.
7. Engleman HM, Asgari-Jirhandeh N, McLeod AL, Ramsay CF, Deary IJ, Douglas NJ. Self-reported use of CPAP and benefits of CPAP therapy: a patient survey. Chest 1996;109:1470-6.
8. Meurice JC, Paquereau J, Neau JP, Caron F, Dore P, Ingrand P, Patte F. Long-term evolution of daytime somnolence in patients with sleep apnea/hypopnea syndrome treated by continuous positive airway pressure. Sleep 1997;20:1162-6.
9. Aguillard RN, Riedel BW, Lichstein KL, Grieve FG, Johnson CT, Noe SL. Daytime functioning in obstructive sleep apnea patients:exercise tolerance, subjective fatigue, and sleepiness. Appl Psychophys Bio 1998;23:207-17.
10. Monasterio C, Vidal S, Duran J, et al. Effectiveness of continuous positive airway pressure in mild sleep apnea-hypopnea syndrome. Am J Respir Crit Care Med 2001;164:939-43.
11. Gotsopoulos H, Chen C, Qian J, Cistulli PA. Oral appliance therapy improves symptoms in obstructive sleep apnea:a randomized, controlled trial. Am J Respir Crit Care Med 2002;166:743-8.
12. Remmers JE, deGroot WJ, Sauerland EK, Anch AM. Pathogenesis of upper airway occlusion during sleep. J Appl Physiol 1978;44:931-8.
13. Tiihonen M, Partinen M. Polysomnography and maintenance of wakefulness test as predictors of CPAP effectiveness in obstructive sleep apnea. Electroencephalogr Clin Neurophysiol 1998;107:383-6.
14. Engleman HM, Kingshott RN, Martin SE, Douglas NJ. Cognitive function in the sleep apnea/hypopnea syndrome (SAHS). Sleep 2000;23:S102-8.
15. Dahlof P, Norlin-Bagge E, Hedner J, Ejnell H, Hetta J, Hallstrom T. Improvement in neuropsychological performance following surgical treatment for obstructive sleep apnea syndrome. Act Oto-Laryngol 2002;122:86-91.
16. Gozal D, Daniel JM, Dohanich GP. Behavioral and anatomical correlates of chronic episodic hypoxia during sleep in the rat. J Neurosci 2001;21:2442-50.
17. Row BW, Kheirandish L, Neville JJ, Gozal D. Impaired spatial learning and hyperactivity in developing rats exposed to intermittent hypoxia. Pediatr Res 2002;52:449-53.
18. Row BW, Liu R, Wei X, Kheirandish L, Gozal D. Intermittent Hypoxia Is Associated with Oxidative Stress And Spatial Learning Deficits in the Rat. Am J Resp Crit Care Med 2003;167:1540-7.
19. Prabhakar NR, Fields RD, Baker T, Fletcher EC. Intermittent hypoxia: cell to system. Am J Phys 2001;281:L524-8.
20. Gu XQ, Haddad GG. Decreased neuronal excitability in hippocampal neurons of mice exposed to cyclic hypoxia. J Appl Physiol 2001;91:1245-50.
21. Pratico D, Uryu K, Leight S, Trojanoswki JQ, Lee VM. Increased lipid peroxidation precedes amyloid plaque formation in an animal model of Alzheimer amyloidosis. J Neurosci 2001;21:4183-7.
22. Castegna A, Thongboonkerd V, Klein JB, Lynn B, Markesbery WR, Butterfield DA. Proteomic identification of nitrated proteins in Alzheimer's disease brain. J Neurochem 2003;85:1394-1401.
23. Beal MF. Oxidatively modified proteins in aging and disease. Free Rad Bio Med 2002;32:797-803.
24. McGinty D, Szymusiak R. Hypothalamic regulation of sleep and arousal. Frontiers in Bioscience 2003;8:s1074-83.
25. Pace-Schott EF, Hobson JA. The neurobiology of sleep: genetics, cellular physiology and subcortical networks. Nature Reviews Neuroscience 2002;3:591-605.
26. Veasey SC, Valladares O, Fenik P, et al. An automated system for recording and analysis of sleep in mice. Sleep 2000;23:1025-40.
27. Benington JH, Kodali SK, Heller HC. Scoring transitions to REM sleep in rats based on the EEG phenomena of pre-REM sleep:an improved analysis of sleep structure. Sleep 1994;17:28-36.
28. Veasey SC, Hsu Y-J, Thayer P, Fenik P. Murine multiple sleep latency test: phenotyping sleep propensity in mice. Sleep 2004, in press.
29. Carskadon MA, Dement WC, Mitler MM, Roth T, Westbrook PR, Keenan S. Guidelines for the multiple sleep latency test (MSLT): a standard measure of sleepiness. Sleep 1986;9:519-24.
30. EEG arousals: scoring rules and examples: a preliminary report from the Sleep Disorders Atlas Task Force of the American Sleep Disorders Association. Sleep 1992;15:173-84.
31. Franken P, Chollet D, Tafti M. The homeostatic regulation of sleep need is under genetic control. J Neurosci 2001;21:2610-21.
32. Uryu K, Laurer H, McIntosh T, et al. Repetitive mild brain trauma accelerates A beta deposition, lipid peroxidation, and cognitive impairment in a transgenic mouse model of Alzheimer amyloidosis. J Neuroscience 2002;22:446-54.
33. Pratico D, Rokach J, Tangirala RK. Brains of aged apolipoprotein E-deficient mice have increased levels of F2-isoprostanes, in vivo markers of lipid peroxidation. J Neurochem 1999;73:736-41.
34. Levine RL, Williams JA, Stadtman ER, Schacter E. Carbonyl assays for determination of oxidatively modified proteins. Methods Enzymol 2000;233:346-57.
35. Frank J, Pompella A, Biesalski HK. Immunohistochemical detection of protein oxidation. Methods Mol Biol 2002;196:35-40.
36. Lorch SA, Foust R, Gow A, et al. Immunohistochemical localization of protein 3-nitrotyrosine and S-nitrocysteine n a murine model of inhaled nitric oxide therapy. Pediatr Res 2000;47:798-805.
37. Gow AJ, McClelland M, Garner SE, Malcolm S, Ischiropoulos H. The determination of nitrotyrosine residues in proteins. Methods Mol Biol 1998;100:291-9.
38. Zhan G, Shaheen F, Mackiewicz M, Fenik P, Veasey SC. Single cell laser dissection with molecular beacon polymerase chain reaction identifies 2A as the predominant serotonin receptor subtype in hypoglossal motoneurons. Neuroscience 2002;113:145-54.
39. Medhurst AD, Harrison DC, Read SJ, Campbell CA, Robbins MJ, Pangalos MN. The use of TaqMan RT-PCR assays for semiquantitative analysis of gene expression in CNS tissues and disease models. J Neurosci Methods 2000;98:9-20.
40. Heinzer R, Gaudreau H, Decary A, Sforza E, Petit D, Morisson F, Montplaisir J. Slow-wave activity in sleep apnea patients before and after continuous positive airway pressure treatment: contribution to daytime sleepiness. Chest 2001;119:1807-13.
41. Ling L, Fuller DD, Bach KB, Kinkead R, Olson EB Jr, Mitchell GS. Chronic intermittent hypoxia elicits serotonin-dependent plasticity in the central neural control of breathing. J Neurosci 2001;21:5381-8.
42. Mitchell GS, Johnson SM. Neuroplasticity in respiratory motor control. J Appl Phys 2003;94:358-74.
43. Peng YJ, Prabhakar NR. Reactive oxygen species in the plasticity of respiratory behavior elicited by chronic intermittent hypoxia. J Appl Phys 2003;94:2342-9.
44. Takakura K, Beckman JS, MacMillan-Crow LA, Crow JP. Rapid and irreversible inactivation of protein tyrosine phosphatases PTP1B, CD45, and LAR by peroxynitrite. Arch Biochem Biophys 1999;369:197-207.
45. Josephs M, Katan M, Rodrigues-Lima F. Irreversible inactivation of magnesium-dependent neutral sphingomyelinase 1 (NSM1) by peroxynitrite, a nitric oxide-derived oxidant. FEBS Letters 2002;531:329-34.
46. van Montfort RL, Congreve M, Tisi D, Carr R, Jhoti H. Oxidation state of the active-site cysteine in protein tyrosine phosphatase 1B. Nature 2003;423:773-7.
47. Gow AJ, Ischiropoulos H. Nitric oxide chemistry and cellular signaling. J Cell Physiol 2001;187:277-82.
48. Ho YS, Liou HB, Lin JK, et al. Lipid peroxidation and cell death mechanisms in pulmonary epithelial cells induced by peroxynitrite and nitric oxide. Arch Toxicol 2002;76:484-93.
49. Droge W. Free radicals in the physiological control of cell function. Physiol Rev 2001;82:47-95.
50. Bao F, Liu D. Peroxynitrite generated in the rat spinal cord induces neuron death and neurological deficits. Neurosci 2002;115:839-49.
51. Fuller DD, Johnson SM, Olson EB, Mitchell GS. Synaptic pathways to phrenic motoneurons are enhanced by chronic intermittent hypoxia after cervical spinal cord injury. J Neurosci 2003;23:2993-3000.
52. Chemelli RM, Willie JT, Sinton CM, et al. Narcolepsy in orexin knockout mice: molecular genetics of sleep regulation. Cell 1999;98:437-51.
53. Parmentier R, Ohtsu H, Djebbara-Hannas Z, Valatx JL, Watanabe T, Lin JS. Anatomical, physiological, and pharmacological characteristics of histidine decarboxylase knock-out mice: evidence for the role of brain histamine in behavioral and sleep-wake control. J Neurosci 2002;22:7695-711.
54. Graves LA, Hellman K, Veasey S, Blendy JA, Pack AI, Abel T. Genetic evidence for a role of CREB in sustained cortical arousal. J Neurophysiol 2003;90:1152-9.
55. Esposito F, Chirico G, Gesualdi NM, et al. Protein kinase B activation by reactive oxygen species is independent of tyrosine kinase receptor phosphorylation and requires SRC activity. J Bio Chem 2003;278:20828-34.
56. Salmeen A, Andersen JN, Myers MP, et al. Redox regulation of protein tyrosine phosphatase 1B involves a sulphenyl-amide intermediate. Nature 2003;423:769-73.
57. Starke DW, Chock PB, Mieyal JJ. Glutathione-thiyl radical scavenging and transferase properties of human glutaredoxin (thioltransferase). Potential role in redox signal transduction. J Bio Chem 2003;278:14607-13.
58. Wendt S, Schlattner U, Wallimann T. Differential effects of peroxynitrite on human mitochondrial creatine kinase isoenzymes. Inactivation, octamer destabilization, and identification of involved residues. J Bio Chem 2003;278:1125-30.
59. Klotz LO, Schroeder P, Sies H. Peroxynitrite signaling:receptor tyrosine kinases and activation of stress-responsive pathways. Free Rad Bio Med 2002;33:737-43.
60. Caselli RJ, Reiman EM, Hentz JG, Osborne D, Alexander GE, Boeve BF. A distinctive interaction between memory and chronic daytime somnolence in asymptomatic APOE e4 homozygotes. Sleep 2002;25:447-53.
61. Grace JB, Walker MP, McKeith IG. A comparison of sleep profiles in patients with dementia with lewy bodies and Alzheimer's disease. Int J Geriatr Psychiatry 2000;15:1028-33.
62. Askenasy JJ. Sleep disturbances in Parkinsonism. J Neurol Trans 2003;110:125-50.